Journal of Structural Geology 33 (2011) 1491–1500

Contents lists available at ScienceDirect

Journal of Structural Geology

journal homepage: www.elsevier.com/locate/jsg

The single-slip hypothesis revisited: Crystal-preferred orientations of sheared quartz aggregates with increasing strain in nature and numerical simulation

L.M. Keller [a,*], M. Stipp [b]

[a] EMPA, Materials Science and Technology, Laboratory for High Performance Ceramics, CH-8400 Dübendorf, Switzerland
[b] Leibniz Institute of Marine Sciences at Kiel University(IFM-GEOMAR), Germany

ARTICLE INFO

Article history:
Received 1 November 2010
Received in revised form
19 July 2011
Accepted 23 July 2011
Available online 30 July 2011

Keywords:
Quartz
Plastic deformation
Crystal-preferred orientation
Natural textures
Model textures

ABSTRACT

This study discusses the fabric development in naturally sheared quartz aggregates in comparison to results from texture modeling according to the polycrystalline plasticity theory with particular emphasis on the formation of a single *c*-axis maximum. The investigated natural shear zone samples were deformed at about 650 ± 50 °C with increasing strain up to $\gamma \approx 14$ and show dynamic recrystallization microstructures of grain boundary migration recrystallization. Neutron diffraction texture analysis results in c-axis pole figures with a single maximum at the periphery of the pole figure. This maximum does not align with the shear plane normal towards higher strain, but rotates towards an inclined orientation in accordance with the sense of shear. Such a rotation is inconsistent with the single-slip hypothesis and suggests that the formation of this *c*-axis pattern is controlled by multi-slip on several slip systems. Based on the polycrystalline plasticity theory, this quartz fabric can develop if combined $\{10\bar{1}1\}\langle 1\bar{2}10\rangle$ {r}<a>, $\{\bar{1}011\}\langle 1\bar{2}10\rangle$ {z}<a> and $\{10\bar{1}1\}\langle 1\bar{2}10\rangle$ prism<a> slip dominates and must not be related to the commonly proposed $(0001)\langle 1\bar{2}10\rangle$ basal<a> slip. The multi-slip texture development is in agreement with the shear sense interpretation from the asymmetry between well-defined quartz fabrics and the foliation. For dominant $(0001)\langle 1\bar{2}10\rangle$ basal<a> slip in quartz and $\gamma > 2$, numerical simulations predict a single peripheral maximum perpendicular to the shear plane and two a-maxima with a ~30°-inward position parallel to the shear plane. This simulation corresponds to naturally observed CPO patterns of quartz formed at different deformation conditions and it is in agreement with the single-slip hypothesis. Hence, our combined natural and numerical data suggest that the single-slip hypothesis is a possible explanation for a single *c*(0001)-maximum but not universally true.

1. Introduction

The development of single quartz c-axis maxima in simple shear deformation has been controversially discussed between researchers from texture modeling and those who analyze textures of naturally and experimentally deformed rocks (e.g. Wenk and Christie, 1991; Schmid, 1994). The easy or single-slip hypothesis of c-axis orientations parallel or slightly oblique to the foliation normal was formulated as an explanation for the observed asymmetry between the orientation of the foliation plane and stretching lineation (interpreted as orientation of finite elongation) and the crystallographic preferred orientation (CPO; used synonymous with the term "texture" in this contribution). According to Bouchez et al. (1983), the hypothesis proposes that "for homogeneous deformation of a polycrystal in simple shear, after shear strains of $\gamma > 2$, a CPO results which is comparable to that of a single crystal favorably oriented for slip on the easy-glide system (i.e. slip plane parallel to the shear plane, slip direction parallel to the shear direction)". The hypothesis is supported by results from complete texture analysis of naturally and experimentally deformed aggregates of quartz (e.g. Bouchez et al., 1983; Dell'Angelo and Tullis, 1989; Ralser, 1990) and also other minerals (e.g. Bouchez and Duval, 1982; Schmid et al., 1987). Underlying rationale of the hypothesis is that the stable end orientation maximizes the resolved shear stress on the dominant active slip system (e.g. Schmid and Casey, 1986). Based on this hypothesis most single maximum c-axis pole figures of quartz have so far been interpreted to be formed by dominant slip on a specific glide plane in a specific crystal direction (slip system), whose activation depends on P-T conditions, strain rate, the dynamic recrystallization mechanism, etc. (e.g. Tullis, 2002 for a recent review). Spatial variations of small-scale CPO patterns in a single shear zone were interpreted on the basis of the single-slip hypothesis to suggest that several active slip systems in

* Corresponding author. Tel.: +41 44 823 4824.
E-mail address: Lukas.Keller@empa.ch (L.M. Keller).

0191-8141/$ – see front matter © 2011 Elsevier Ltd. All rights reserved.
doi:10.1016/j.jsg.2011.07.008

fabric domains contribute to the formation of the bulk CPO (e.g. Pauli et al., 1996; Pennacchioni et al., 2010). However, there are only empirical concepts backing the hypothesis and no exhaustive physical theory. In addition, easy-glide failed to be simulated by computer modeling as a steady state process (e.g. Wenk and Christie, 1991).

The choice of the right external reference system is essential for a kinematic and also for a mechanistic interpretation of pole figures. Textures need to be plotted with respect to the shear plane and the shear direction in order to test whether an orientation maximum indicative of a slip system remains stable or rotates with respect to the shear plane. Hence, on the basis of complete orientation data it may be proofed if texture maxima rotate or become fixed along a deformation path of progressive simple shear that is for example unclear for quartz (Burg and Laurent, 1978; Lister and Williams, 1979; Carreras and Garcia Celma, 1982). Recent shear experiments on quartzite showed that towards higher strain a *c*-axis maximum is formed at the periphery of the pole figure, which rotates away from the shear plane normal in accordance with the sense of shear (Heilbronner and Tullis, 2006). Strictly speaking, such a rotation is inconsistent with the single-slip hypothesis predicting an alignment of the *c*-axis parallel to the shear plane normal towards higher strain (e.g. Bouchez et al., 1983).

In order to further illuminate this long-term controversy we will present the strain-dependent texture development of naturally deformed quartz bands from a shear zone with known structural relationships and physical conditions of deformation. Then, we will compare the measured texture development to both the single-slip hypothesis and predictions made on the basis of the polycrystalline plasticity theory. Finally, the influence of dynamic recrystallization on the formation of single c-axis maxima during shearing will be discussed in the context of our microstructural results, computer modeling and texture data from other studies.

2. Investigated samples

The samples come from a shear zone (Fig. 1) that was formed in polymetamorphic metapelites from the Monte Rosa nappe (Central Alps, N-Italy). It is part of a network of anastomosing shear zones where only domains as wide as 10 m are unaffected by Alpine deformation and preserve a pre-Alpine foliation (Keller et al., 2004, their Fig. 2a). The new Alpine foliation within central parts of the shear zone is parallel to the main foliation of the frontal part of the Monte Rosa nappe and can laterally be traced for several hundreds of meters (Keller et al., 2004, their Fig. 1c). Together with the gradual deflection of the pre-Alpine foliation (Fig. 1) there is a gradual change in mineralogy from the pre-Alpine garnet-biotite-plagioclase-kyanite schist to a garnet-white-mica-schist in the Alpine shear zone. Synkinematic metamorphic conditions during texture formation were about 12.5 kbar and 650 ± 50 °C and fluid present conditions (Keller et al., 2004).

Four samples of the shear zone were analyzed: sample 1 represents the undeformed stage and samples 2, 3 and 4 document progressive stages during shear deformation (Fig. 1). Concerning the geometrical relationships between the measured CPOs and the shear zone geometry we consider the pre-Alpine foliation in the undeformed wall rock as passive marker plane, which is progressively rotated into parallelism with the shear zone (Fig. 1). The orientation of the new Alpine foliation in the center of the shear zone is regarded as reasonable approximation of the orientation of the shear plane (Fig. 1). The observed stretching lineation is perpendicular to an axis around which the pre-Alpine foliation is dragged into parallelism to the shear zone (Keller and Schmid, 2001). This indicates that the strain field of our shear zone is close to heterogeneous simple shear and the sinistral shear sense is in accordance with small-scale shear sense indicators (Keller and Schmid, 2001). For simple shear, the shear strain γ at constant volume may be given by $\gamma = \cot \alpha' - \cot \alpha$ (Ramsay, 1980), where α is the angle between a passive plane and the shear plane prior to deformation and α' is the angle after deformation. Implicit in this approach is the assumption of constant volume during deformation. Mass balance considerations related to syn-deformational metamorphism suggest a volume loss <20% during deformation (Keller et al., 2004). Thus, strain estimates are considered as upper limits and the angle α' is regarded as a function of both the shear strain γ and the volume change. Because strain estimates are affected by large errors resulting from the uncertainties in measuring small angles, an error range of $\pm 3°$ for α' is assumed (Fig. 1). Particular at higher strain the uncertainties result in large errors and strain estimates should be treated with caution.

The investigated pure quartz bands show pinch-and-swell structures and some boudinage indicating that the quartz bands are rheologically stronger than the micaceous matrix of the shear zone. Despite this rheological difference, microscale strain partitioning structures cannot be observed suggesting that both, quartz bands and matrix, were intensely deformed during Alpine deformation. Furthermore, the strong increase in texture maxima as presented below shows an increased deformation of the quartz bands with increasing strain towards the center of the shear zone. Hence, the deformation of the quartz bands is clearly related to the Alpine shearing and controlled by the kinematic framework of the shear zone.

3. Methods

Bulk textures of minerals were measured using the multi-detector neutron time of flight diffractometer (HIPPO) at the Los

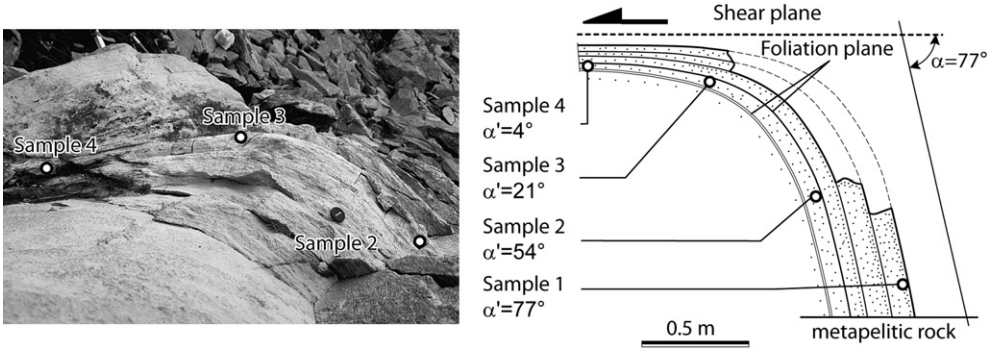

Fig. 1. Photograph and sketch of the investigated shear zone with locations of the four quartz band samples within the metapelitic host rock. Angles between shear plane and original respective rotated foliations are indicated as α and α' and are used to calculate the shear strain of the samples (see text and Fig. 2).

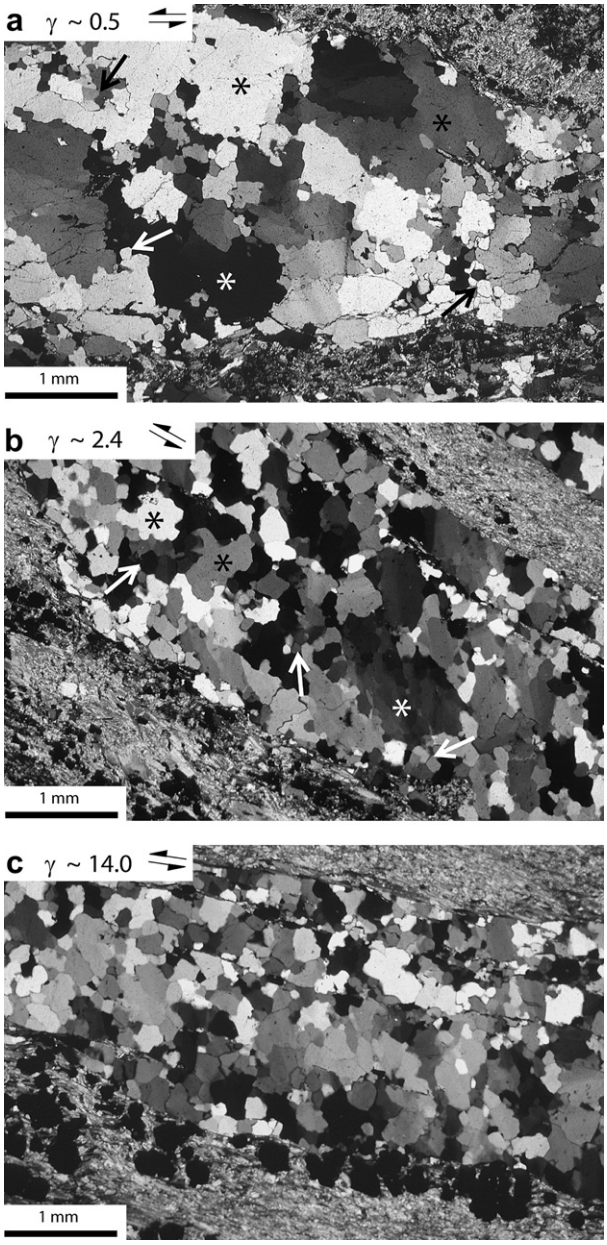

Fig. 2. Micrographs of the three progressively deformed quartz veins (crossed polarizers) from the shear zone shown in Fig. 1. Samples were cut perpendicular to the foliation and parallel to the stretching lineation. Trend of the foliation/lineation is parallel to the long edge of the image (a and c) and slightly rotated (b) in order to increase the orientation contrast between the grains. Shear strain γ, shear sense and scale are indicated for the three images. Microstructures of second phase minerals in the host rock are ignored here. a) Quartz microstructure with an irregular and wide grain size distribution ranging from large grains in millimeter-scale (porphyroclasts) to small grains of about 100 μm (newly recrystallized grains?). The quartz band has a variable width and an irregular boundary to the main foliation of the host rock. Large grains (stars) show amoeboid grain shapes with lobate grain boundaries and dissection microstructures as well as intracrystalline deformation features (e.g. some undulose and patchy extinction). Small grains (arrows) show equant grain shapes and no internal deformation structures (sample 2). See text for further explanation and discussion. b) Quartz microstructure with a more narrow grain size distribution ranging from larger grains of some hundred micrometer in diameter (relict porphyroclasts?) to small grains of about 100 μm. The larger grains (stars) show variable sizes, irregular shapes, and boundaries as well as intracrystalline deformation features (e.g. some patchy extinction and subgrains). Small grains (arrows) show equant grain shapes and no internal deformation structures. Quartz band width and boundary to the main foliation of the host rock are quite constant and straight (sample 3). c) Quartz microstructure with a narrow grain size distribution similar to b. Large grains tend to be a little more irregular in shape and boundary trend than small grains. Intracrystalline deformation features are rare. Quartz band width and boundary to the main foliation of the host rock are quite constant and straight (sample 4).

Alamos Neutron Science Center (Wenk et al., 2003). HIPPO data were analyzed by Rietveld texture analysis implemented in the software package MAUD (e.g. Lutterotti et al., 1999; http://www.ing.unitn.it/~maud/). The analyzed samples are cubes of a size of approximately 0.7 cm^3 consisting of 4–6 mm thick foliation-parallel quartz bands of the metapelite. Quartz-rich portions were selected or when not available were glued together so that at least 60 volume percent quartz with high grain statistics were attained. Apart from quartz, the samples contain also micas, garnet and accessory minerals.

4. Microstructures and textures

The deformation microstructures of the foliation-parallel quartz bands, presumably original quartz veins, are indicative of dynamic recrystallization of quartz at high metamorphic temperatures (Fig. 2). With increasing strain towards the shear zone center dynamic recrystallization is associated with an overall grain size reduction. The weakly deformed sample 2 consists of large and irregularly shaped porphyroclasts with lobate grain boundaries and dissection microstructures (Fig. 2a). Second phase minerals like mica grains are included in some of these porphyroclasts and do not pin grain boundaries. The porphyroclast microstructure can be interpreted as being relic of the host rock and is typical for grain boundary migration recrystallization (GBM II of Stipp et al., 2002a). Undulose and patchy extinction within the porphyroclasts, optical subgrains and recrystallized grains of about the same or a slightly larger size (~100 μm) may be related to shear zone formation (Fig. 2a).

At intermediate strain (sample 3, Fig. 2b) the large porphyroclasts with amoeboid grain shape and millimeter-size are not present. Slightly irregularly shaped grains of a size of a few 100 μm may be relic porphyroclasts. Some of these grains show polygonization by internal subgrains (Fig. 2b). The latter are of the size or slightly smaller than the second group of grains in the quartz band. These fairly equant grains (~100 μm) are presumably recrystallized by progressive subgrain rotation recrystallization. Because of the quite continuous grain size distribution it can be assumed that the once recrystallized grains grew by successive grain boundary migration recrystallization. Indeed, with increasing size the grains have a more and more irregular shape with lobate grain boundaries proving this assumption (Fig. 2b).

The highest strain sample 4 (Fig. 2c) shows a microstructure, which is very similar to the one of sample 3. Only the large irregularly shaped grains are further diminished and smaller in size and there are correspondingly more small and equant grains. Microstructural development and grain size distribution of the three samples suggest that sample 4 is completely or at least nearly completely recrystallized. Boundaries of the dynamically recrystallized quartz grains are locally pinned by e.g. micas indicating grain boundary migration hindered by second phase particles (GBM I of Stipp et al., 2002a). So, it can be concluded that dynamic recrystallization in the shear zone is charcterized by grain size reducing subgrain rotation followed by grain boundary migration recrystallization.

The quartz c(0001), a{11$\bar{2}$0}, m(10$\bar{1}$0), r(10$\bar{1}$1), z(10$\bar{1}$1) -pole figures of the four samples are presented in Fig. 3. The undeformed sample 1 shows a broad and weak maximum of *c*-axes. This texture may be inherited from the undeformed host rock. The low strain sample 2 displays a single girdle c-axis fabric with main maxima close to the center and a secondary maximum close to the periphery of the pole figure. Related a-, m-, r-, and z-pole figures of samples 1 and 2 are in general accordance to the c-axis fabrics, but very weak and diffuse and therefore not further described here (Fig. 3). At higher strain (samples 3 and 4) the c-axis CPO develops

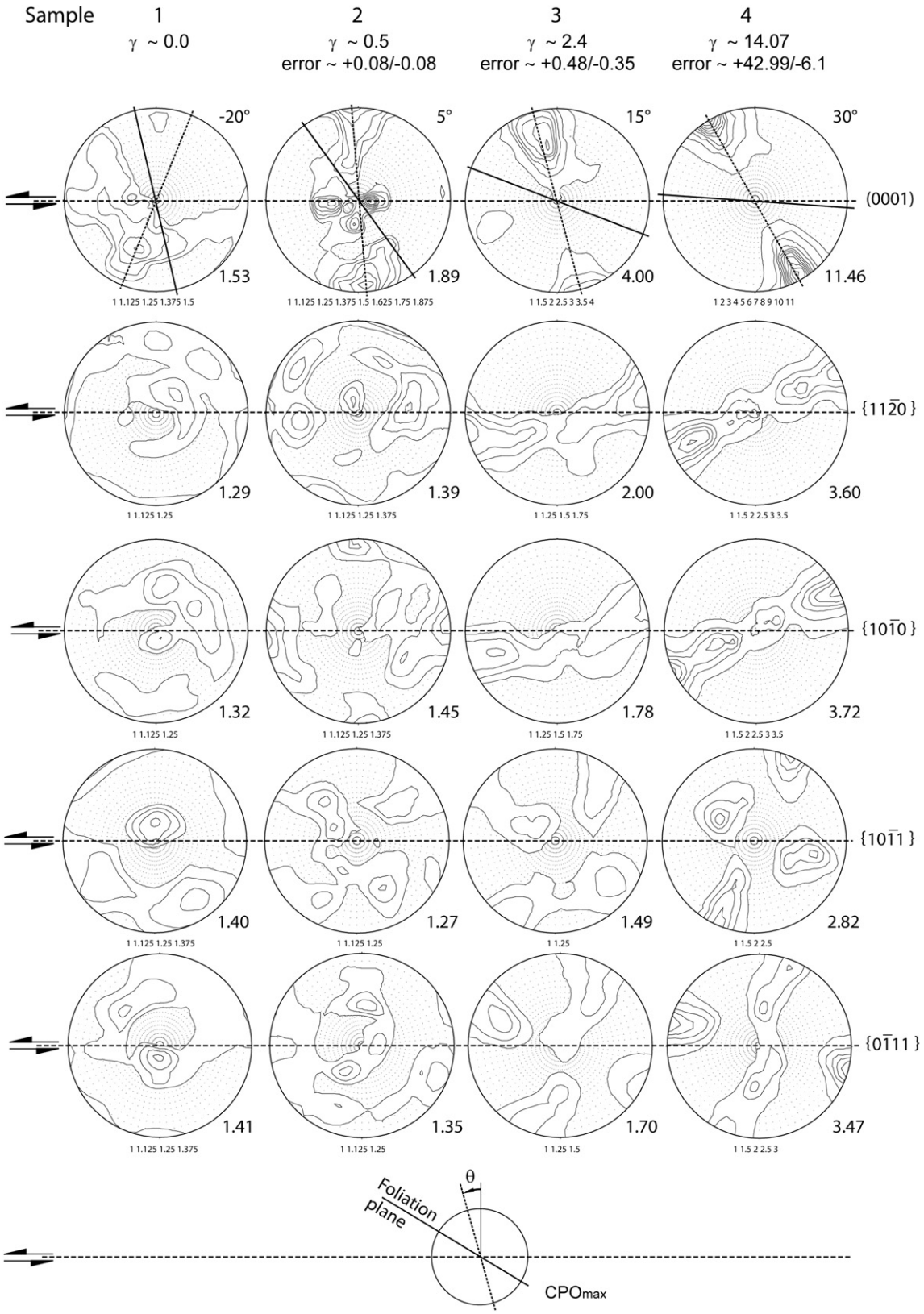

Fig. 3. c(0001), a{11$\bar{2}$0}, m(10$\bar{1}$0), r(10$\bar{1}$1}, z(10$\bar{1}$1), -pole figures of sheared quartz bands from the shear zone (see Fig. 1). From left to right, the samples show a quartz texture development with increasing simple shear strain from $\gamma \approx 0$ to $\gamma \approx 14$. Shear plane is horizontal and shear sense is sinistral in the pole figures; the dashed and the solid lines indicate the fabric skeleton axis and the foliation, respectively. The rotation angle, θ, of the fabric skeleton axis is given at upper right of the c -pole figures. Shear strain for the three progressively deformed samples (2, 3, 4) is calculated by assuming an error of $\pm 3^\circ$ for α'. Pole figures are contoured in intervals of multiples times uniform distribution indicated below each plot (equal area projection) with magnitude of maximum (CPO_{max}) at lower right. See text for further explanation.

to an increasingly sharper and stronger peripheral maximum, which is inclined with respect to the shear plane and shows an apparent rotation with the sense of shear (Fig. 3). Correspondingly, the basal plane represented by the a-axis and m-pole figures rotates with increasing strain and sense of shear. For the intermediate strain sample 3, for which the c-axis maximum is approximately 30° inwards displaced, the a-axis maximum is at the periphery and the m-pole maximum in a 30°-inclined related position. In contrast, for the high strain sample 4, for which the c-axis maximum is at the periphery, the m-pole maximum is at the periphery and the a-axis maximum in a 30°-inclined related position (Fig. 3). The r- and z-pole maxima of sample 3 indicate that the rhomb planes are nearly parallel and perpendicular to the foliation (20-30°-rotated). The r-pole figure of sample 4 displays three maxima, suggesting that one r-plane is subparallel and two are nearly perpendicular to the foliation, while the z-pole maximum is subparallel to the stretching lineation.

5. Modeling of crystal preferred orientations

In order to simulate the measured texture development of quartz we used the code version 7c of the viscoplastic self-consistent model, which was provided by R. Lebensohn, Los Alamos National Laboratory, USA. The VPSC model (e.g. Molinari et al., 1987) allows the prediction of CPOs developed under different deformation conditions. One model assumption is that the grains of a polycrystal deform by slip only. In the VPSC model each crystal grain is considered as an inclusion, which only maintains stress equilibrium and strain compatibility with a "homogenous equivalent medium" whose behavior is identical to the macroscopic behavior of the polycrystal. In contrast to classical modeling approaches that impose either strain compatibility (i.e. upper bound; Taylor, 1938) or stress equilibrium (lower bound; Sachs, 1928) within the polycrystal, the VPSC model allows strain rate and stress of an individual grain to differ from the corresponding quantities of the polycrystal.

For our simulations we used an initial aggregate consisting of 2000 randomly oriented grains, which were deformed during 200 steps resulting in a final equivalent shear strain of $\gamma = 4$. The input parameters are the slip systems of quartz, their critical resolved shear stress (CRSS) and strain rate sensitivity (i.e. stress exponent). Studies on the creep behavior of quartz indicate a low stress exponent ranging typically between 3 and 4 (e.g. Paterson and Luan, 1990; Gleason and Tullis, 1995; Hirth et al., 2001). The VPSC model is not very sensitive to variations in the stress exponent ranging between 3 and 5. An increase of the stress exponent only increases the magnitude of the CPO maximum for any given finite strain. Hence, the stress exponent for all considered 15 slip systems (i.e.$(0001)\langle 1\bar{2}10\rangle$ basal<a>, $\{\bar{1}0\bar{1}0\}[0001]$ prism[c], $\{10\bar{1}1\}\langle 1\bar{2}10\rangle$ {r}<a>, $\{\bar{1}011\}\langle 1\bar{2}10\rangle$ {z}<a>, and $\{10\bar{1}0\}\langle 1\bar{2}10\rangle$ prism<a>) was set to 3. As pointed out below, the only sensitive and adjustable parameter in the VPSC model is therefore the CRSS for the different slip systems.

Regarding the VPSC concept it should be noted that no stable end orientation is ever attained because all crystal orientations rotate at any instant of time and with different rotation rates. Therefore, texture evolution in terms of the VPSC concept reflects different rotation rates: fast rotating crystals "catch up" with slow rotating orientations and together they successively form an increasingly stronger maximum close to the slow rotating orientation.

6. Modeling results and discussion

Insights into the relation between the orientation of crystallographic fabrics of quartz and the kinematic framework associated with progressive simple shear can be obtained by studying the CPO evolution of quartz in naturally formed shear zones. The CPO evolution of quartz generally appears to follow either of two trends (see Lister and Williams, 1979 and references therein): the CPO remains constant (e.g., Pennacchioni et al., 2010) or it rotates with respect to the shear plane (e.g., Law et al., 2010). The latter case is supported by the presented natural samples (Fig. 3) and also by shear experiments on quartzites (Dell'Angelo and Tullis, 1989; Heilbronner and Tullis, 2006). In the experiments of Heilbronner and Tullis (2006), the single *c*-axis maximum at the periphery of the pole figure does also not align with the shear plane normal towards higher strain, but in fact rotates with the sense of shear towards an inclined orientation in accordance with the sense of shear. This finding is not consistent with the single-slip hypothesis. Consequently, an alternative explanation for the observed CPO development must be found. Taking the large number of reported slip systems in quartz into account (e.g., Christie et al., 1964; Baëta and Ashby, 1969; Hobbs et al., 1972; Tullis et al., 1973; Blacic, 1975; Twiss, 1976; Linker et al., 1984; Hobbs, 1985; Blumenfeld et al., 1986), it is reasonable to assume that multi-slip on several slip systems led to the observed CPO development.

In order to test this multi-slip hypothesis, we modeled the observed texture development during simple shear of a quartz aggregate using the VPSC model and setting the CRSS of the most important slip systems to similar values (= model A). Alternatively, the same modeling approach but with one preferred slip system accommodating most of the shear strain was used to test if the single-slip hypothesis is a possible scenario (= model B). In the case of the presented quartz fabric it is suggested that slip occurred predominantly along the $(0001)\langle 1\bar{2}10\rangle$ basal $<$ a $>$ slip system. In that way the consistency of the single-slip hypothesis with the crystal plasticity theory can be proved.

To simulate the observed texture development we changed the CRSS during repeated calculation until we obtained good agreement between calculated and observed textures (model A in Fig. 4). Good agreement was obtained by setting rhomb<a> and prism<a> as dominant systems (CRSS = 1) and basal<a> (CRSS = 3) and prism<c> (CRSS = 2) harder. To test the single-slip hypothesis within the polycrystalline plasticity theory in a second model (model B in Fig. 4), the chosen CRSS assures that basal<a> slip (CRSS = 1) is the dominant active slip system in comparison to the other systems (CRSS = 3). Fig. 4 presents calculated *c*-axis and a-axis pole figures of quartz for the models A and B. Fig. 5 shows a diagram displaying the relative activity of the considered slip systems and the numbers of activated slip systems.

6.1. Results of Model A

Model A results in c- and a-axis fabrics which correspond to the natural fabrics at higher strain ($\gamma > 2$). The peripheral c-axis maximum rotates with the sense of shear towards an increasingly sharper maximum that is inclined with the shear plane (Fig. 4). In addition, the peripheral *a*-axis maximum develops. Note, that this maximum is not aligned with the shear direction. $\{\bar{1}011\}\langle 1\bar{2}10\rangle$ {r}<a> slip and $\{10\bar{1}1\}\langle 1\bar{2}10\rangle$ {z}<a> slip followed by$\{10\bar{1}0\}\langle 1\bar{2}10\rangle$ prism<a> slip are the dominant active slip systems and the number of active slip systems (with activity of >5%) ranges between 9 and 7 throughout the deformation history with a decreasing tendency (Fig. 5). Such a behavior is in agreement with the fact that the deformation occurred at relative high temperatures of around 650 °C and that at these temperatures and for geological reasonable strain rates, the $\{\bar{1}011\}\langle 1\bar{2}10\rangle$ {r}<a> and $\{10\bar{1}0\}\langle 1\bar{2}10\rangle$ prism<a> slip systems are similarily easy to activate as $(0001)\langle 1\bar{2}10\rangle$ basal<a> slip (Hobbs et al., 1972; Nicolas and Poirier, 1976; Hobbs, 1985).

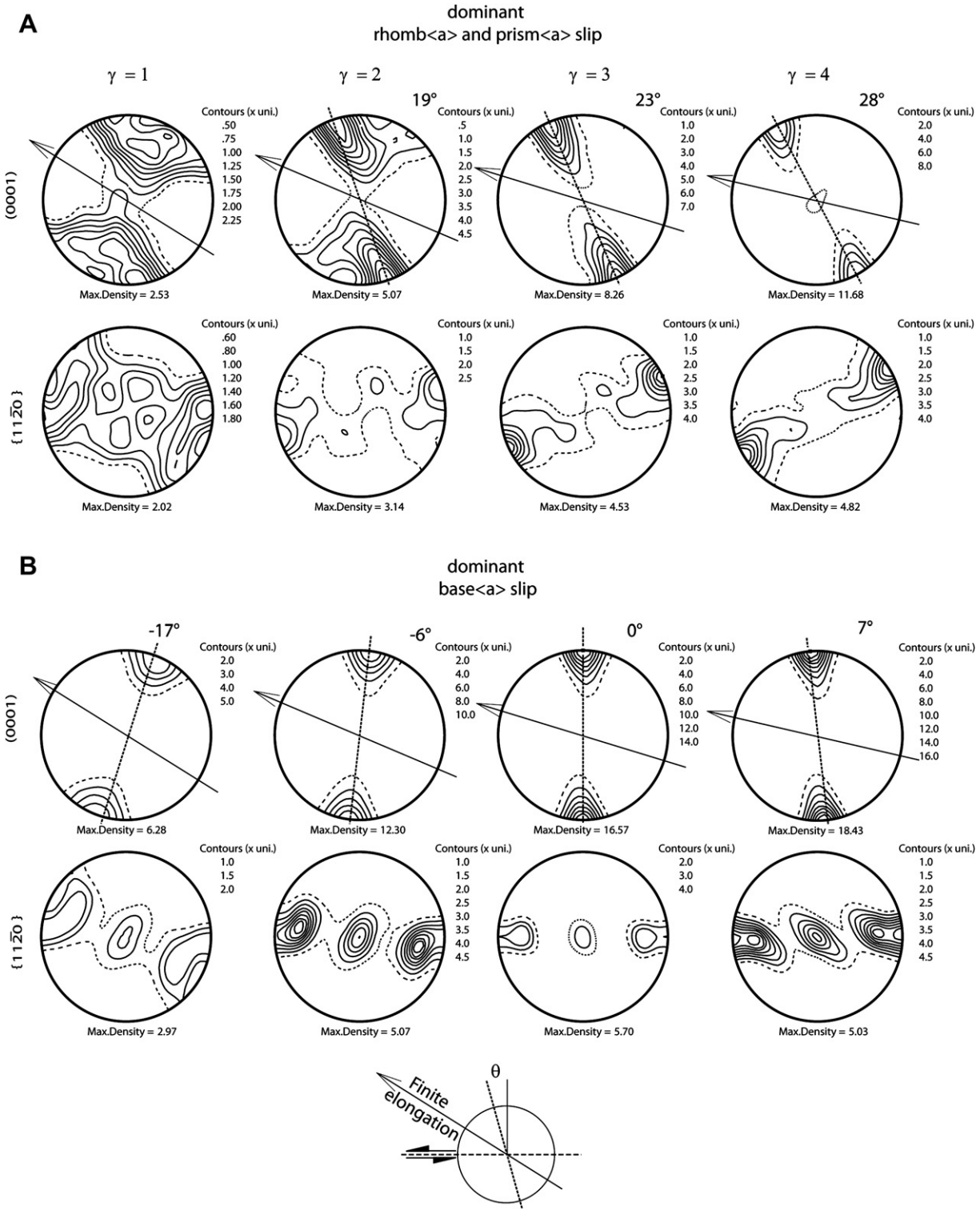

Fig. 4. Two model results (model A and B, see text for further explanation) from viscoplastic self-consistent (VPSC) modeling showing the c(0001)-axis and a{11-20}-axis fabrics of quartz after a shear strain γ of 1, 2, 3 and 4. Shear plane is horizontal, shear sense is sinistral, the arrow-line shows the orientation of finite elongation and the dashed line indicates the fabric skeleton axis. The rotation angle θ of the fabric skeleton axis is given at the upper right of the c -pole figures. Pole figures are contoured in intervals of multiples times uniform distribution indicated in the contours' scale to the right of each plot (equal area projection) with magnitude of maximum (CPO_{max}) below the pole figures. Lowest contour level is a dashed line.

6.2. Results of Model B

For dominant $(0001)\langle 1\bar{2}10\rangle$ basal<a> slip, VPSC simulations predict the formation of a peripheral *c*-axis maximum perpendicular to the shear plane and the alignment of the basal plane parallel to the shear plane towards higher shear strains with a $\sim 30^{\circ}$ inwards position of the a-axis maxima (Fig. 4). Such a CPO of quartz has been observed for porphyroclastic ribbon grains in the Tonale mylonites

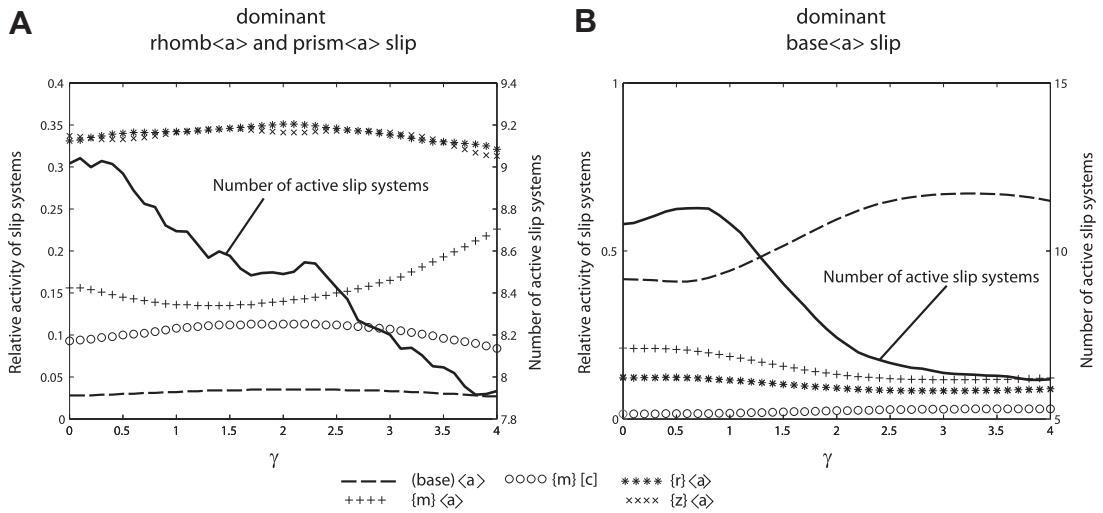

Fig. 5. Relative activity of the considered slip systems and number of active slip systems from the VPSC models A and B of Fig. 4 plotted versus the shear strain. R-and z-rhomb <a> and prism <a> slip are dominant in model A, basal <a> slip is dominant in model B (see text for further discussion).

(samples 13-1 and 14-5 of Fig. 6) which dynamically recrystallized by subgrain rotation recrystallization below 500 °C (Stipp et al., 2002a). The large ribbon grains in these samples are extremely elongated in two dimensions with a long to short axis ratio of 20:1 or even more. This elongation together with the strong texture suggests a kind of single-slip or easy-glide mechanism on the basal plane for the ribbon grains. Strain compatibility for the ribbon grains may be maintained by dynamic recrystallization and further deformation of the newly recrystallized grains. The recrystallized grains show girdle-type fabrics indicative of multi-slip deformation (Fig. 6; see also Stipp et al., 2002a). Hence, easy or single-slip may be feasible for ribbon grains in the zone of dominant subgrain rotation

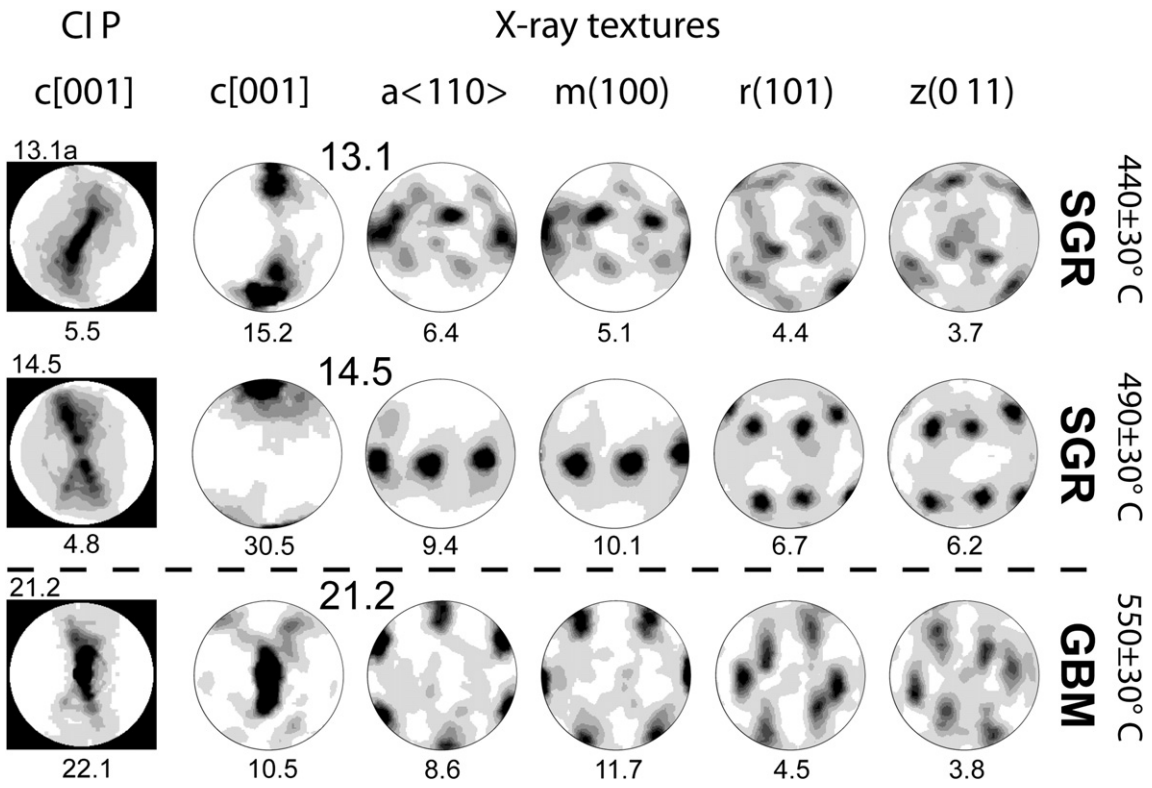

Fig. 6. Pole figures from sheared quartz veins of the Tonale line measured by Computer Integrated Polarization microscopy (CIP) and X-ray goniometry measurements (from Stipp et al., 2002a). Deformation temperature and dominant dynamic recrystallization mechanism are indicated. Pole figures are shaded in 0.5 intervals up to 4x uniform, magnitudes of maxima are given below pole figures. Sections are perpendicular to the foliation and parallel to the stretching lineation (XZ sections, with X horizontal); bulk shear sense of samples is dextral. CIP [c]-axis pole figures relate to recrystallized grains only; 13.1a represents a pole figure of a smaller section representing a more localized texture (fabric domain). X-ray goniometry results are bulk textures. For samples 13.1 and 14.5, pole figures reflect textures of porphyroclasts (volume proportion of the porphyroclasts is more than 50%), for sample 21.2 those of recrystallized grains (volume proportion of the recrystallized grains is more than 85%).

recrystallization and so preferentially lower temperature shearing than the here presented shear zone samples with GBM microstructures. Large porphyroclastic ribbon grains potentially deformed by easy or single-slip are also characteristic for bulging recrystallization at even lower temperature deformation (e.g. van Daalen et al., 1999; Stipp et al., 2002a; Stipp and Kunze, 2008).

Pole figures of shear experiments on ice and norcamphor also correspond to the modeling results because for both materials the *c*-axis tend to align perpendicular to the shear plane towards higher strain (Bouchez and Duval, 1982; Herwegh et al., 1997). Furthermore, the simulations display an asymmetry between CPO and SPO (i.e. finite elongation) at higher strain that is in accordance with the sense of shear. Hence, the results of model B are consistent with the predictions made by the single-slip hypothesis. In agreement with previous modeling studies (e.g. Wenk and Christie, 1991), the simulations show a single *c*-axis maximum with apparent rotation against the sense of shear at low shear strain. Such a rotation is not inconsistent with the single-slip hypothesis, which is exclusively defined for higher strains ($\gamma > 2$; e.g. Bouchez et al., 1983). However, there is some disagreement, because two $(0001)\langle 1\bar{2}10\rangle$ basal<a> slip systems align at an angle of $\sim 30^{\circ}$ symmetrically to the shear direction in the VPSC simulations. This suggests that in a polycrystalline quartz aggregate, in which deformation occurs largely along the $(0001)\langle 1\bar{2}10\rangle$ basal<a> slip system, the shear strain is accommodated by two crystallographically equivalent slip systems, whose slip directions tend to align as close to the shear direction as possible. Indeed, the a-axis pole figures of the porphyroclastic ribbon grains of samples 13-1 and 14-5 (Fig. 6) show a-axis maxima not parallel to the stretching lineation but slightly inclined to it, whereas m-pole maxima are located at the periphery of the pole figure and parallel or nearly parallel to the stretching lineation. In addition, the number of active slip systems in model B is always higher than 5 even in the case when $(0001)\langle 1\bar{2}10\rangle$ basal<a> slip accounts for more than 70% of the shear strain above $\gamma \approx 2.5$ (Fig. 5). Nevertheless, basal<a> slip is so predominant and increases even further towards higher strain that the calculated pole figures of model B at higher strain can be described by the term 'easy-glide on the basal plane'.

6.3. The effects of dynamic recrystallization

While dynamic recrystallization during shear zone formation is far from completion in the low strain sample 2, it presumably progresses to near completion in the high strain sample 4. Dynamic recrystallization occurred at water-present conditions (Keller et al., 2004) within dominant GBM, which is indicative of high temperature and/or slow strain rate deformation (i.e. low flow stress deformation; Stipp et al., 2002b). The microstructural development from low to high strain, however, indicates that apart from grain boundary migration, which allows grains to grow, presumably subgrain rotation and subsequent recrystallization were active to attain a new equilibrium microstructure at a smaller recrystallized grain size. Hence, the microstructural reworking of the sample set is characterized by the interaction of subgrain rotation and grain boundary migration recrystallization, whereas subgrain rotation dominating at early strain increments is replaced by an increasing contribution of grain boundary migration with increasing strain.

Comparable to the c-axis pole figure change towards a strong maximum in the center of the pole figure (Y-maximum) which occurs at the transition from dominant SGR to GBM in Fig. 6 (Stipp et al., 2002a) we expect the development of a Y-maximum indicative of dominant prism <a>slip with increasing strain. Such a texture development would be in accordance to what has been observed for high temperature quartz deformation (e.g. Schmid and Casey, 1986; Stipp et al., 2002a; Mancktelow and Pennacchioni, 2004) and to the high temperature experiments of Heilbronner and Tullis (2006). Indeed, Y-maximum textures have been determined by Keller and Schmid (2001) in mylonites formed at the same deformation phase and adjacent to the investigated shear zone. The strain cannot be estimated in these mylonites because they do not show any relationship to the pre-existing fabric. Their main foliation is, however, parallel to the shear plane indicating the accommodation of a higher finite strain than the one of sample 4.

Not only the amount of strain but also differences in the strain path (variable contributions of pure shear to the assumed simple shear deformation) could be the reason why the texture development of the investigated shear zone deviates from other natural

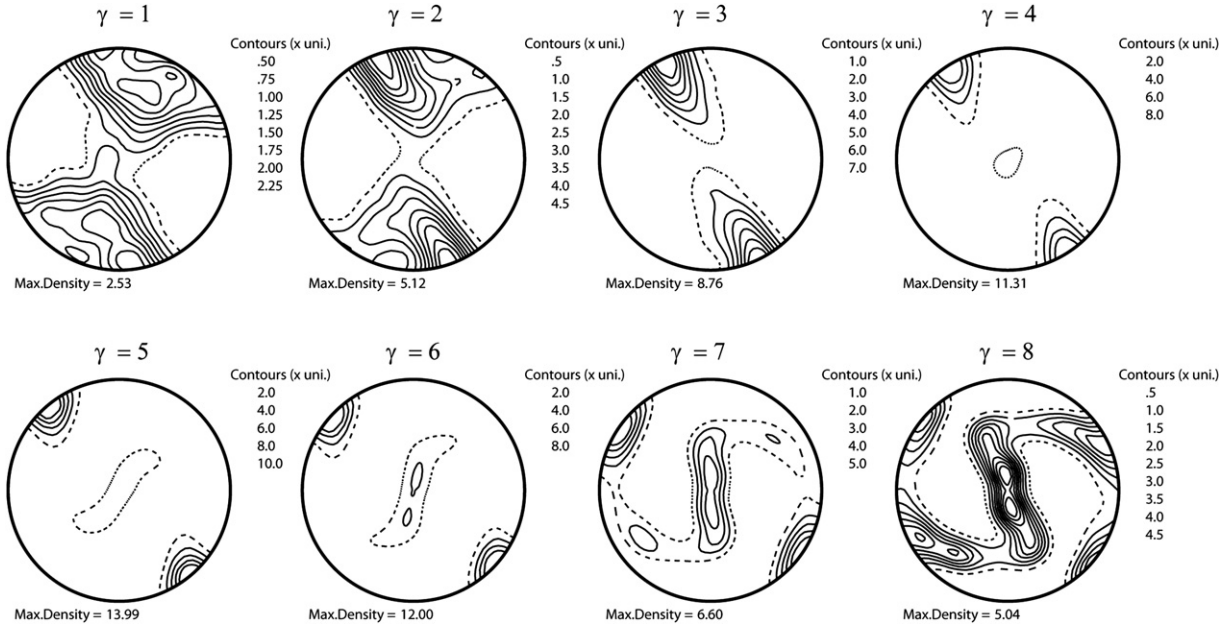

Fig. 7. *c*-axis texture evolution up to a strain $\gamma = 8$ simulated with the VPSC model and by including a recrystallization routine (see text for explanation). The critical resolved shear stress (CRSS) values are those from model A (see text and Fig. 3). Shear plane is horizontal, shear sense is sinistral.

examples and the switch towards a Y-maximum c-axis pole figure in the numerical simulations and the experiments of Heilbronner and Tullis (2006). A pure shear component in the latter experiments, for example, is one possible reason for the texture differences between these experiments and the simulations with a transition to a dominant Y-maximum (Fig. 7).

Stipp et al., 2002a interpreted their texture transition from girdle-type fabrics to a c-axis maximum in Y as a switch from multi-slip to dominant prism <a>slip enabled by grain boundary migration recrystallization ensuring strain compatibility. In contrast, the VPSC modeling inherently suggests that multi-slip within all the grains fulfills the von Mises criterion up to the highest strain, and our simulations predict predominant shearing in <a>-direction on rhomb and prism planes.

In order to account for dynamic recrystallization the used VPSC code can be modified by inclusion of a recrystallization routine. In that routine the most strongly deformed grains split into subgrains, when the aspect ratio between grain long and short axis reaches a critical value (see Beyerlein et al., 2003, for the employed fragmentation model). Hence, this parameter represents a critical strain dependence and controls the onset of recrystallization as dominant process for the texture development. For our simulations the critical aspect ratio value was arbitrarily set to 10. The simulation results based on this value and the slip systems of model A, however, are in agreement with the experiments of Heilbronner and Tullis (2006) which showed that recrystallization has strong influence on the texture for $\gamma > 4$ and shifts the c-axis to the center of the pole figure (Fig. 7). The most strongly deformed grains accumulate in the center of the pole figure. They recrystallize fast and/or maintain a low internal energy via dislocation creep and related transport of dislocations to the grain boundaries. During continuous deformation, grains with low internal strain energy are supposed to consume grains with higher strain energy from different orientations by grain boundary migration. Hence, ongoing shearing within GBM may shift the *c*-axes towards the center of the pole figure and stabilizes this end orientation at higher shear strain. In that respect, our VPSC modeling results are comparable to earlier work applying Taylor-Bishop-Hill-modeling and a plastic rheology which indicates the formation of strong point maxima (Jessell and Lister, 1990). An explanation for the delay in texture development in our natural sample set in comparison to the modeling including recrystallization is that plastic deformation by dislocation glide is relatively easy and dynamic recrystallization less effective when there are two or more equally soft slip systems active (e.g. Model A, Fig. 5; Kaminski and Ribe, 2001).

Other reasons why our shear zone samples do not show the texture transition at even higher strain values than our VPSC simulations and the experiments of Heilbronner and Tullis (2006) could be manifold. First of all, finite strain values bear large errors and are difficult to correlate between nature, experiment and numerical modeling. Second, the obliteration or rotation of the pre-existing fabrics may require a higher amount of shear strain than the transformation of initially random fabrics of the experimental starting material and the numerical simulation. This is demonstrated by the high strain sample 4 which is not yet aligned with the shear plane. Third, additional parameters (e.g., temperature, strain rate, water content, strain path) may control dynamic recrystallization (cf. Stipp et al., 2006) and texture development in combination with strain. Hence, it appears that much more must be learned about the involved physical parameters and processes until texture development can be satisfyingly understood. Nevertheless, apart from the discrepancies in texture development at high strain there is great agreement between the experiments of Heilbronner and Tullis (2006), our natural samples and the VPSC model at low strain displaying the development of a single peripheral *c*-axis maximum in accordance to the sense of shear.

7. Summary and conclusions

The CPO development of quartz in a natural high-temperature shear zone displays the formation of a single *c*-axis maximum at the periphery of the pole figure. Thereby, the *c*-axis maximum does not align with the shear plane normal towards higher strain, but in fact rotates with the sense of shear towards an inclined orientation. Regarding high-temperature shearing of quartz aggregates, such a rotation is inconsistent with the single-slip hypothesis and alternatively suggests that deformation involves a number of simultaneously active slip systems. Corresponding texture modeling on the basis of the polycrystalline plasticity theory shows the development of the same quartz fabric if combined $\{10\bar{1}1\}\langle 1\bar{2}10\rangle$ {r}<a>, $\{\bar{1}011\}\langle 1\bar{2}10\rangle$ {z}<a>, and $\{10\bar{1}0\}\langle 1\bar{2}10\rangle$ prism<a> slip dominates instead of the commonly interpreted $(0001)\langle 1\bar{2}10\rangle$ basal<a> slip. Our new interpretation is in accordance with the sense of shear and hence with the use of asymmetric c-axis fabrics as shear sense indicator. In contrast, a peripheral single c-axis maximum in low temperature quartz mylonites with a large content of strongly deformed porphyroclastic ribbon grains implies that the related CPO development is controlled by dominant basal glide on two crystallographically equivalent $(0001)\langle 1\bar{2}10\rangle$ basal<a> slip systems. According to their simulated high predominance and the little contribution of other slip systems this texture can further be interpreted as the result of easy-glide on the basal plane.

Acknowledgements

We would like to thank H. R. Wenk for introducing the first author into VPSC modeling and the use of BEARTEX and also for his comments on an early version of the manuscript. We thank R. Lebensohn from Los Alamos National Laboratory for providing the latest version of the VPSC code. S. Vogel from Los Alamos Neutron Science Center kindly carried out the neutron texture measurements. M. Voltolini is thanked for patiently helping with MAUD and K. Ullemeyer for his help with pole figure plotting. Comments by S.M. Schmid and the reviews by G. Pennacchioni and P. Xypolias and the journal editor R.E. Holdsworth are gratefully acknowledged.

References

Baëta, R.D., Ashby, K.H.G., 1969. Slip systems in quartz: I. experiments. American Mineralogist 54, 1551–1573.
Beyerlein, I.J., Lebensohn, R.A., Tome, C.N., 2003. Modeling of texture and microstructural evolution in the equal channel angular process. Material Sciences and Engineering A345, 122–138.
Blacic, J.D., 1975. Plastic-deformation mechanisms in quartz: the effect of water. Tectonophysics 27, 271–294.
Blumenfeld, P., Mainprice, D., Bouchez, J.L., 1986. C-slip in quartz from subsolidus deformed granite. Tectonophysics 127, 97–115.
Bouchez, J.L., Duval, P., 1982. The fabric of polycrystalline ice deformed in simple shear: experiments in torsion, natural deformation and geometrical interpretation. Textures and Microstructures 5, 171–190.
Bouchez, J.L., Lister, G.S., Nicolas, A., 1983. Fabric asymmetry and shear sense in movement zones. Geologische Rundschau 72, 401–419.
Burg, J.P., Laurent, P., 1978. Strain analysis of a shear zone in a granodiorite. Tectonophysics 47, 15–42.
Carreras, J., Garcia Celma, A., 1982. Quartz of c-axis fabric variation at the margins of a shear zone developed in schists from Cap de Creus (Spain). Acta Geologica Hispanica 17, 137–149.
Christie, J.M., Griggs, D.T., Carter, N.L., 1964. Experimental evidence for basal slip in quartz. Journal of Geology 72, 734–756.
Dell'Angelo, L.N., Tullis, J., 1989. Fabric development in experimentally sheared quartzites. Tectonophysics 169, 1–21.
Gleason, G.C., Tullis, J., 1995. A flow law for dislocation creep of quartz aggregates determined with the molten salt cell. Tectonophysics 247, 1–23.
Heilbronner, R., Tullis, J., 2006. Evolution of c axis pole figures and grain size during dynamic recrystallization: results from experimentally sheared quartzite. Journal of Geophysical Research 111, B10202. doi:10.1092/2005JB004194.

Herwegh, M., Handy, M.R., Heilbronner, R., 1997. Temperature- and strain-rate-dependent microfabric evolution in monomineralic mylonite: evidence from in situ deformation of norcamphor. Tectonophysics 280, 83–106.

Hirth, G., Teyssier, C., Dunlap, W.J., 2001. An evaluation of quartzite flow laws based on comparisons between experimentally and naturally deformed rocks. International Journal of Earth Sciences 90, 77–87.

Hobbs, B.E., McLaren, A.C., Paterson, M.S., 1972. Plasticity of single crystals of synthetic quartz. In: Heard, H.C., Borg, I.Y., Carter, N.L., Raleigh, C.B. (Eds.), Flow and Fracture of Rocks, 16. Geophysical Monograph, pp. 29–53.

Hobbs, B.E., 1985. The geological significance of microfabric analysis. In: Wenk, H.-R. (Ed.), Preferred Orientation in Deformed Metals and Rocks: An Introduction to Modern Texture Analysis. Academic Press, Orlando, pp. 463–484.

Jessell, M.W., Lister, G.S., 1990. A simulation of the temperature dependence of quartz fabrics. In: Knipe, R.J., Rutter, E.H. (Eds.), Deformation Mechanisms, Rheology and Tectonics. Geological Society Special Publication, vol. 54, pp. 353–362.

Kaminski, E., Ribe, N.M., 2001. A kinematic model for recrystallization and texture development in olivine polycrystals. Earth and Planetary Science Letters 189, 253–267.

Keller, L.M., Schmid, S.M., 2001. On the kinematics of shearing near the top of the Monte Rosa nappe and the nature of the Furgg zone in Val Loranco (Antrona valley, N. Italy): tectonometamorphic and paleogeographic consequences. Swiss Bulletin of Mineralogy and Petrology 81, 347–367.

Keller, L.M., Abart, R., Stünitz, H., De Capitani, C., 2004. Deformation, mass transfer and mineral reactions in an eclogite facies shear zone in a polymetamorphic metapelite (Monte Rosa nappe, western Alps). Journal of Metamorphic Geology 22, 97–118.

Law, R.D., Mainprice, D., Casey, M., Lloyd, G.E., Knipe, R.J., Cook, B., Thigpen, J.R., 2010. Moine thrust zone mylonites at the Stack of Glencoul: I - microstructures, strain and influence of recrystallization on quartz crystal fabric development. In: Law, R.D., Butler, R.W.H., Holdsworth, R., Krabbendam, M., Strachan, R.A. (Eds.), Continental Tectonics and Mountain Building - The Legacy of Peach and Horne. Geological Society, London, Special Publication, vol. 335, pp. 543–577. 10.144/SP335.23.

Linker, M.F., Kirby, S.H., Ord, A., Christie, J.M., 1984. Effects of compression direction on the plasticity and rheology of hydrolytically weakened synthetic quartz crystals at atmospheric pressure. Journal of Geophysical Research 89 (NB6), 4241–4255.

Lister, G.S., Williams, P.F., 1979. Fabric development in shear zones: theoretical controls and observed phenomena. Journal of Structural Geology 1, 283–297.

Lutterotti, L., Matthies, S., Wenk, H.-R., 1999. MAUD: a friendly Java program for material analysis using diffraction. IUCr: Newsletter of the CPD 21, 14–15.

Mancktelow, N.S., Pennacchioni, G., 2004. The influence of grain boundary fluids on the microstructure of quartz-feldspar mylonites. Journal of Structural Geolology 26, 47–69.

Molinari, A., Canova, G.R., Azhy, S., 1987. A self-consistent approach of large deformation crystal polycrystal viscoplasticity. Acta Metallurgica 35, 2983–2994.

Nicolas, A., Poirier, J.P., 1976. Crystalline Plasticity and Solid State Flow in Metamorphic Rocks. John Wiley & Sons, London, pp. 444.

Paterson, M.S., Luan, F.C., 1990. Quartzite rheology under geological conditions. In: Knipe, R.J., Rutter, E.H. (Eds.), Deformation Mechanisms, Rheology and Tectonics. Special Publications of the Geological Society of London, 54, pp. 299–307.

Pauli, C., Schmid, S.M., Panozzo Heilbronner, R., 1996. Fabric domains in quartz mylonites: localized three dimensional analysis of microstructure and texture. Journal of Structural Geology 18, 1183–1203.

Pennacchioni, G., Menegon, L., Leiss, B., Nestola, F., Bromiley, G., 2010. Development of crystallographic preferred orientation and microstructure during plastic deformation of natural coarse-grained quartz veins. Journal of Geophysical Research 115 (B12405), 23.

Ralser, S., 1990. Shear zones developed in an experimentally deformed quartz mylonite. Journal of Structural Geology 12, 1033–1045.

Ramsay, J.G., 1980. Shear zone geometry: a review. Journal of Structural Geology 2, 83–99.

Sachs, G., 1928. Zur Ableitung einer Fließbedingung. Zeitung des Vereins deutscher Ingenieure 72, 734–736.

Schmid, S.M., 1994. Textures of geological materials: computer model predications versus empirical interpretations based on rock deformation experiments and field studies. In: Bunge, H.J., Siegesmund, S., Skrotzki, W., Weber, K. (Eds.), Texture of Geological Materials. DGM, Informationsgesellschaft Verlag, pp. 179–301.

Schmid, S.M., Casey, M., 1986. Complete fabric analysis of some commonly observed quartz c-axis patterns. In: Hobbs, B.E., Heard, H.C. (Eds.), Mineral and Rock Deformation: Laboratory Studies – The Patterson Volume, 36. American Geophysical Union, Geophysical Monograph, pp. 161–199.

Schmid, S.M., Panozzo, R., Bauer, S., 1987. Simple shear experiments on calcite rocks: rheology and microfabric. Journal of Structural Geology 9, 747–778.

Stipp, M., Kunze, K., 2008. Dynamic recrystallization near the brittle-plastic transition in naturally and experimentally deformed quartz aggregates. Tectonophysics. doi:10.1016/j.tecto.2007.11.041 TECTO124034.

Stipp, M., Stünitz, H., Heilbronner, R., Schmid, S.M., 2002a. The eastern Tonale fault zone: a "natural laboratory" for crystal plastic deformation of quartz over a temperature range from 250°C to 700°C. Journal of Structural Geology 24, 1861–1884.

Stipp, M., Stünitz, H., Heilbronner, R., Schmid, S.M., 2002b. Dynamic recrystallization of quartz: correlation between natural and experimental conditions. In: De Meer, S., Drury, M.R., De Bresser, J.H.P., Pennock, G.M. (Eds.), Deformation Mechanisms, Rheology and Tectonics: Current Status and Future Perspectives. Geological Society of London, Special Publications, 200, pp. 171–190.

Stipp, M., Tullis, J., Behrens, H., 2006. Effect of water on the dislocation creep microstructure and flow stress of quartz and implications for the recrystallized grain size piezometer. Journal of Geophysical Research 111. doi:10.1029/2005JB003852 B04201.

Taylor, G.I., 1938. Plastic strain in metals. Journal of the Institute of Metals 62, 307–324.

Tullis, J., 2002. Deformation of granite rocks: experimental studies and natural examples. In: Shun-Ichiro, K., Wenk, H.R. (Eds.), Plastic Deformation of Minerals and Rocks, 51. Reviews in mineralogy and geochemistry, pp. 51–95.

Tullis, J., Christie, J.M., Griggs, D.T., 1973. Microstructures and preferred orientations of experimentally deformed quartzites. Geological Society American Bulletin 84, 297–314.

Twiss, R.J., 1976. Some planar deformation features, slip systems, and submicroscopic structures in synthetic quartz. Journal of Geology 84, 701–724.

van Daalen, M., Heilbronner, R., Kunze, K., 1999. Orientation analysis of localized shear deformation in quartz fibres at the brittle-ductile transition. Tectonophysics 303, 83–107.

Wenk, H.R., Christie, J.M., 1991. Comments on the interpretation of deformation textures in rocks. Journal of Structural Geology 13, 1091–1110.

Wenk, H.R., Lutterotti, L., Vogel, S., 2003. Texture analysis with the new HIPPO TOF diffractometer. Nuclear Instruments Methods A515, 575–588.